Separation Science and Technology
Publication details, including instructions for authors and subscription information:
http://www.informaworld.com/smpp/title~content=t713708471

Electrical Aspects of Adsorbing Colloid Flotation. XVI. Double-Layer Relaxation

P. C. Sundareswaran[a]; David J. Wilson[a]
[a] DEPARTMENT OF CHEMISTRY, VANDERBILT UNIVERSITY, NASHVILLE, TENNESSEE

To cite this Article Sundareswaran, P. C. and Wilson, David J.(1983) 'Electrical Aspects of Adsorbing Colloid Flotation. XVI. Double-Layer Relaxation', Separation Science and Technology, 18: 6, 555 — 570
To link to this Article: DOI: 10.1080/01496398308060294
URL: http://dx.doi.org/10.1080/01496398308060294

SEPARATION SCIENCE AND TECHNOLOGY, 18(6), pp. 555–570, 1983

Electrical Aspects of Adsorbing Colloid Flotation. XVI. Double-Layer Relaxation

---

P. C. SUNDARESWARAN and DAVID J. WILSON

DEPARTMENT OF CHEMISTRY
VANDERBILT UNIVERSITY
NASHVILLE, TENNESSEE 37235

Abstract

A mathematical model for studying relaxation processes in the electric double layer adjacent to a plane charged surface is developed and analyzed. The model is nonlinear and nonideal. A time constant of roughly 7×10^{-8} s qualitatively describes the relaxation processes. Increased applied potentials yield nonlinear responses, which are investigated by Fourier analysis. The effects of ionic size are determined. The relaxation rate is fast enough so that the local equilibrium assumption in foam flotation is amply justified.

INTRODUCTION

Adsorptive bubble separation techniques (*1, 2*) have shown considerable promise for the recovery of trace elements for analysis (*3, 4,* for example), the separation of valuable metals from leachates (*5, 6*), the removal of toxic metals and other pollutants from wastewaters (*7–12*), and for a number of other applications. Two recent reviews are by Grieves (*13*) and Wilson and Clarke (*14*), and a monograph has also recently appeared on ore flotation (*15*).

We have been interested in the application of electric double-layer theory to precipitate and adsorbing colloid flotation (*16–20*), and have used a nonideal model to calculate the differential capacitance of the double layer (*21*). We have also estimated the time constants involved in the diffusion of floc particles to the air–water interfaces of bubbles in the presence of an electric double layer (*22, 23*). These calculations, however, all assumed that the electric double layers themselves were always at equilibrium with the

0149-6395/83/1806-0555$3.50/0

surface potentials in their vicinities. In the following we analyze the validity of this assumption by providing a method for calculating the relaxation rate of a nonideal electric double layer. We do this by calculating the frequency dependence of the amplitude and phase shift of the double-layer's differential capacitance in the presence of a sinusoidally varying applied potential, and by examining the time dependence of the surface charge density associated with the ionic atmosphere under the influence of a step potential.

ANALYSIS

We take as our starting point the following equations:

$$\frac{d^2\psi}{dx^2} = \frac{-\psi\pi\rho}{D} \tag{1}$$

where x = distance from the planar electrode on the left, to which the periodic potential is to be applied
$\psi = \psi(x, t)$ = electric potential at the point x at time t
ρ = charge density
D = dielectric constant of water

$$\rho = ze[c^+(x, t) - c^-(x, t)] \tag{2}$$

where $|ze|$ = |charge| on anions and cations
c^+ = cation concentration, ions/cm^3
c^- = anion concentration

Also,

$$\mu^+(x, t) = ze\psi + kT \log_e \left[\frac{c^+ c_{\max}}{c_{\max} - (c^+ + c^-)}\right] \tag{3}$$

$$\mu^-(x, t) = -ze\psi + kT \log_e \left[\frac{c^- c_{\max}}{c_{\max} - (c^+ + c^-)}\right] \tag{4}$$

where $\mu^+(x, t)$ = chemical potential of cations (anions) at the point x at time t

$\dfrac{c_{\max}}{c_{\max} - (c^+ + c^-)}$ = activity coefficient to correct for the finite volumes of the anions and cations

Here we have dropped μ_0^+ and μ_0^- since we shall subsequently be dealing only with differences.

The diffusion of the ions is governed by

$$\frac{\partial c^+}{\partial t} = \frac{1}{6\pi r\eta}\frac{\partial}{\partial x}\left(c^+ \frac{\partial \mu^+}{\partial x}\right) \tag{5}$$

and

$$\frac{\partial c^-}{\partial t} = \frac{1}{6\pi r\eta}\frac{\partial}{\partial x}\left(c^- \frac{\partial \mu^-}{\partial x}\right) \tag{6}$$

where r = effective ionic radius of anions and cations
η = viscosity of water

We substitute Eq. (2) into Eq. (1) and integrate to obtain

$$\frac{\partial \psi}{\partial x}(x, t) = \frac{-4\pi z e}{D}\int_0^x [c^+(x', t) - c^-(x', t)]dx' + C_1(t) \tag{7}$$

where

$$C_1 = \frac{\partial \psi}{\partial x}(0, t) = -\frac{4\pi\sigma(t)}{D} \tag{8}$$

Here $\sigma(t)$ is the total surface charge density; Eq. (8) results from the requirement of electrical neutrality.

A second integration then yields

$$\psi(x, t) = \frac{-4\pi z e}{D}\int_0^x \int_0^{x'} [c^+(x'', t) - c^-(x'', t)]dx''dx' + C_1(t)x + C_2(t) \tag{9}$$

The boundary condition at $x = 0$,

$$\psi(0, t) = \psi_0 + \psi_1 \sin \omega t \tag{10}$$

yields

$$C_2(t) = \psi_0 + \psi_1 \sin \omega t \tag{11}$$

We also require that

$$\psi(l, t) = 0 \tag{12}$$

where l is the distance between the left electrode and a grounded electrode on the right. This permits us to determine $C_1(t)$ from Eqs. (9) and (11):

$$C_1(t) = \frac{1}{l}\left\{-\psi_0 - \psi_1 \sin \omega t + \frac{4\pi z e}{D} \int_0^l \int_0^{x'} [c^+(x'', t) - c^-(x'', t)]\, dx''dx'\right\} \tag{13}$$

If we interchange the order of integration in Eqs. (9) and (13), we can carry out the first integrals; we illustrate with Eq. (9):

$$\psi(x, t) = \frac{-4\pi z e}{D} \int_0^x \int_{x''}^x [c^+(x'', t) - c^-(x'', t)]\, dx'dx'' + C_1 x + C_2 \tag{14}$$

$$= \frac{-4\pi z e}{D} \int_0^x (x - x'')[c^+(x'', t) - c^-(x'', t)]\, dx'' + C_1 x + C_2 \tag{15}$$

We next digress briefly to verify that Eq. (15) does indeed give us the correct potential in the case where the solution is ideal, $ze\psi$ is small compared to kT, and the double layer has come to equilibrium with a surface potential at $x = 0$ of ψ_0. For this case

$$\psi(x) = \psi_0 \exp(-\kappa x) \tag{16}$$

where

$$\kappa^2 = c_\infty 8\pi z^2 e^2 / DkT \tag{17}$$

We have

$$c^+ = c_\infty \exp\left(\frac{-ze\psi}{kT}\right) \tag{18}$$

$$c^- = c_\infty \exp\left(\frac{ze\psi}{kT}\right) \tag{19}$$

These are expanded in series through linear terms in ψ and substituted into Eq. (15) to yield

$$\psi(x) = \kappa^2 \int_0^x (x - x'')\psi(x'')\, dx'' + C_1 x + C_2 \tag{20}$$

Differentiate with respect to x to get

$$\frac{d\psi}{dx} = \kappa^2 (x - x'')\psi(x'')\,|_{x''=x} + \kappa^2 \int_0^x \psi(x'') dx'' + C_1$$

$$= \kappa^2 \int_0^x \psi(x'')\, dx'' + C_1 \tag{21}$$

Differentiate again to obtain

$$\frac{d^2\psi}{dx^2} = \kappa^2 \psi \tag{22}$$

which has Eq. (16) as the desired solution.

Since our coupled equations include some which are highly nonlinear, to make further progress we must proceed numerically. We do so as follows. We let

$$\psi_i(t) = \psi(x_i, t), \qquad i = 1, 2, \ldots, N$$

$$x_i = (i - 1/2)\Delta x$$

which we calculate by approximating Eq. (15) by the discrete sum,

$$\psi_i(t) = \frac{-4\pi z e}{D} \sum_{m=1}^{i} (i + 1 - m)[c_m^+ - c_m^-](\Delta x)^2 + C_1 x_i + C_2 \tag{23}$$

The representation for $C_1(t)$ as a discrete sum is given by

$$C_1(t) = \frac{1}{l}\left\{ - \psi_0 - \psi_1 \sin \omega t \right.$$

$$\left. + \frac{4\pi z e}{D} \sum_{m=1}^{N} (N + 1 - m)[c_m^+ - c_m^-](\Delta x)^2 \right\} \tag{24}$$

The differential equations governing the driven diffusion of the ions, Eqs. (5) and (6), are given by

$$\frac{dc_i}{dt} = \frac{1}{\Delta x^2 6\pi\eta r}\left[\frac{c_{i+1}+c_i}{2}(\mu_{i+1}-\mu_i) + \frac{c_{i-1}+c_i}{2}(\mu_{i-1}-\mu_i)\right] \qquad (25)$$

where $c_i = c_i^+$ or c_i^-, and $\mu_i = \mu_i^+$ or μ_i^-.

At the ends of the interval we have

$$\frac{dc_1}{dt} = \frac{1}{\Delta x^2 6\pi\eta r}\frac{c_2+c_1}{2}(\mu_2-\mu_1) \qquad (26)$$

$$\frac{dc_N}{dt} = \frac{1}{\Delta x^2 6\pi\eta r}\frac{c_{N-1}+c_N}{2}(\mu_{N-1}-\mu_N) \qquad (27)$$

We integrate these equations forward in time by means of a standard predictor-corrector method of the following form.

Starter:

$$y^*(\Delta t) = y(0) + y'(0)\,\Delta t \qquad (28)$$

Predictor:

$$y^*[(n+1)\,\Delta t] = y[(n-1)\,\Delta t] + y'(n\,\Delta t)\cdot 2\Delta t \qquad (29)$$

Corrector:

$$y[(n+1)]\,\Delta t = y(n\,\Delta t) + \{y'(n\,\Delta t) + y'[(n+1)\,\Delta t]\}\cdot 1/2\,\Delta t \qquad (30)$$

The new concentrations [at time $(n+1)\,\Delta t$] are then used to calculate the $\psi_i[(n+1)\,\Delta t]$ from Eq. (23). $C_1[(n+1)\,\Delta t]$ is then recalculated from Eq. (24). $C_2[(n+1)\,\Delta t]$ is recalculated from Eq. (11), and the surface charge density associated with the electric double layer is calculated from

$$\sigma(t) = \frac{ze}{l}\int_0^l \int_0^{x'} [c^+(x'', t) - c^-)x'', t)]\,dx''dx' \qquad (31)$$

$$= \frac{ze}{l}\sum_{m=1}^{N}(N+1-m)|c_m^+ - c_m^-|\,\Delta x^2 \qquad (32)$$

One needs to estimate a value for l; this is done by calculating the Debye length

$$\kappa^{-1} = (8\pi z^2 e^2 c_\infty / DkT)^{-1/2} \tag{33}$$

and then setting l equal to $J\kappa^{-1}$, where $J \geq 5$ to 10.

The viscosity and dielectric constant of water vary markedly with temperature; these are calculated by means of Eqs. (34) and (35):

$$\eta(T) = \eta_{20} \cdot \exp\left\{ -\frac{(T - T_{20})[a + b(T - T_{20})]}{T - c} \right\} \tag{34}$$

where $T_{20} = 293.15$ deg
$c = 164.15$ deg
$a = 3.15507$
$b = 1.926 \times 10^{-3}\ \text{deg}^{-1}$
$\eta_{20} = 0.01005$ poise
$\eta(T) =$ viscosity at T(°K), poise

$$D(T) = D_{25} + (T - T_{25})[\alpha + \beta(T - T_{25})] \tag{35}$$

where $D_{25} = 78.54$
$T_{25} = 298.15$ deg
$\alpha = -0.361187\ \text{deg}^{-1}$
$\beta = 0.68921 \times 10^{-3}\ \text{deg}^{-2}$

Equation (34) is given by Atkins (*24*), and Eq. (35) was obtained by making a least-squares quadratic fit to the reported (*25*) data.

The equilibrium surface charge density associated with the ionic atomosphere is given by (*21*):

$$\sigma_{\text{eq}} = \frac{-\psi_0}{|\psi_0|} \frac{D}{4\pi} \left[\frac{8\pi kT}{D} c_{\max} \log_e \frac{1 + B \cosh(ze\psi_0/kT)}{1 + B} \right]^{1/2} \tag{36}$$

$$B = \frac{2c_\infty}{c_{\max} - 2c_\infty} \tag{37}$$

for the model we are using. This result allows one to avoid long numerical integrations when examining the response of the double layer to a step potential.

The first few Fourier coefficients of the expansion of $\sigma(t)$ were determined for the runs made at 25 MHz. The Fourier series was fitted to $\sigma(t)$ over the interval 0.90×10^{-7} s $\leq t \leq 1.30 \times 10^{-7}$ s, by which time the initial transients had died out; Simpson's rule was used to do the integrations. The coefficients were given by

$$c_0 = \sum_{j=0}^{40} \sigma[(90 + j)\Delta t] \cdot h_j/40 \tag{38}$$

$$c_n = \sum_{j=0}^{40} \sigma[(90 + j) \cdot \Delta t] \cdot \cos(2\pi nj/40) \cdot h_j/20 \tag{39}$$

$$S_n = \sum_{j=0}^{40} \sigma[(90 + j)\ \Delta t) \cdot \sin(2\pi nj/40) \cdot h_j/20 \quad n = 1, 2, 3 \tag{40}$$

$$h_0 = h_{40} = 1/3,\ h_2 = h_4 = \cdots = 4/3,\ h_1 = h_3 = \cdots = 2/3$$

The phase shift and amplitude of the first Fourier component of $\sigma(t)$ were then calculated by

$$\phi_1 = \arctan(-s_1/c_1) \tag{41}$$

and

$$a_1 = (s_1^2 + c_1^2)^{1/2} \tag{42}$$

RESULTS

A computer program to solve this model was written and run on a DEC 1099 computer. A number of runs were made in which a voltage step was applied at $t = 0$ and the response of the surface charge density of the ionic atmosphere was determined. Some results showing the effects of varying the ionic strength of the electrolyte solution are given in Fig. 1. We see the expected increase in capacitance with increasing ionic strength, and also find that the response time of $\sigma(t)$ decreases very markedly with increasing ionic strength. This is presumably because formation of the ionic atmosphere requires movement of the ions for shorter distances in the more concentrated solutions.

Another possible voltage input to the system is a rectangular pulse; we see the resulting output displayed in Fig. 2. Such an input could be used to get estimates of σ_{equil} and a time constant for the approach of the double layer to equilibrium. Obtaining more than one time constant from these curves is made difficult, however, by the fact that real exponentials do not constitute an orthonormal set.

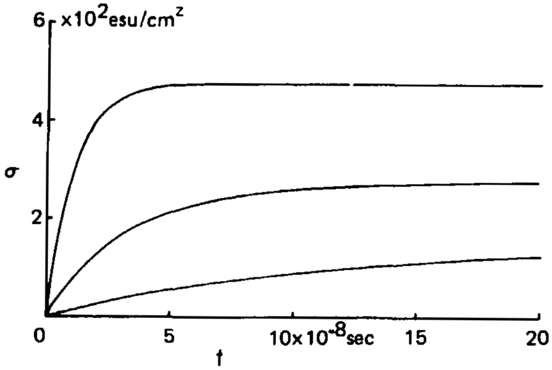

FIG. 1. Response of $\sigma(t)$ to a step voltage. Effects of ionic strength. $\psi(0) = 0$, $t < 0$; $\psi(0) = 10$ mV, $t \geq 0$. $r = 2$ Å; $T = 298$ K; $z = 1$; $c_{\max} = 10$, $c_\infty = 0.03$, 0.01, 0.003 mol/L (top to bottom); $\eta = .0089613$ P; $D = 78.594$.

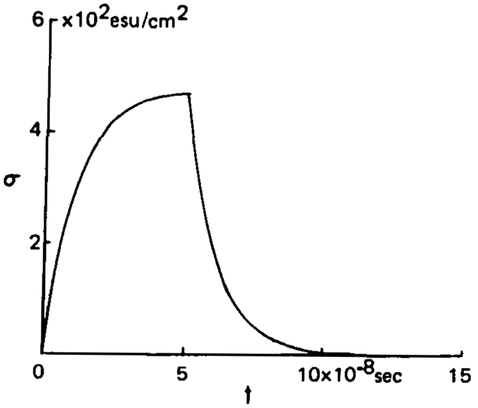

FIG. 2. Response of $\sigma(t)$ to a rectangular voltage pulse. $c_\infty = 0.03$ mol/L; $\psi(0) = 0$, $t < 0$; $\psi(0) = 10$ mV, $0 \leq t \leq 5 \times 10^{-8}$ s; $\psi(0) = 0$, $t > 5 \times 10^{-8}$ s. Other parameters as in Fig. 1.

TABLE 1
Fourier Coefficients for a Run in the Linear Range
($\nu = 25$ MHz, other parameters as in Fig. 3)

$c_0 = 0.16443 \times 10^{-1}$ esu/cm^2
$c_1 = 0.11928 \times 10^{3}$
$s_1 = 0.20348 \times 10^{3}$
$c_2 = 0.23094 \times 10^{-2}$
$s_2 = 0.94447 \times 10^{-2}$
$c_3 = 0.51577 \times 10^{-2}$
$a_1 = 0.23586 \times 10^{3}$
$\phi_1 = 59.622^\circ$

The easy experimental availability of sinusoidally varying input voltages of the form

$$\psi(t) = \psi_0 + \psi_1 \sin 2\pi\nu t \tag{43}$$

and the ease of Fourier analyzing the output function $\sigma(t)$ to investigate nonlinear responses of the double layer suggests that such sinusoidal input voltages should be of particular interest. For these reasons the bulk of our runs were made with such input voltages.

One set of runs was made with $\psi_0 = 0$, $\psi_1 = 10$ mV, and ν varying from 1.5625 to 100 MHz by powers of $\sqrt{2}$. At voltages this small, one expects the system to exhibit a quite linear response, with negligible contributions from higher harmonics in the Fourier series for $\sigma(t)$. This is shown to be the case by results presented in Table 1 for a run made at 25 MHz. Fourier coefficients of the fundamental frequency are four orders of magnitude large than any of the others.

Plots of these low voltage runs at 6.25 and 50 MHz are shown in Figs. 3 and 4, and qualitatively exhibit the expected increase in phase angle and decrease in amplitude of $\sigma(t)$ with increasing frequency. The dependence of phase angle on frequency for these small signal runs is shown in Fig. 5; ϕ_1 shows the expected increase from values slightly larger than zero to values slightly less then 90° as we increase the frequency by a factor of 64 (from 1.5625 to 100 MHz). The sigmoid curve exhibits no unusual structure. A plot of the magnitude of the capacitance $(\sigma(t)_{\max}/\psi_{\max})$ is given in Fig. 6; it exhibits a decrease by a factor of about seven over the frequency range studied, with no unusual features.

Another set of runs was made with an input voltage of 10 $(1 + \sin 2\pi\nu t)$ mV; the plots of ϕ and capacitance versus frequency were indistinguishable from those shown in Figs. 5 and 6.

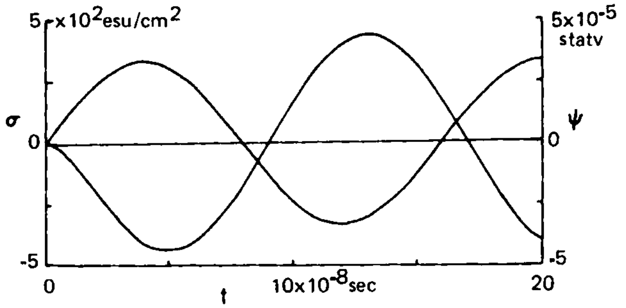

FIG. 3. Response of $\sigma(t)$ to a small, low-frequency sinusoidal voltage. $\psi(0) = 10$ mV·sin $2\pi\nu t$, $\nu = 6.25$ MHz, other parameters as in Fig. 2.

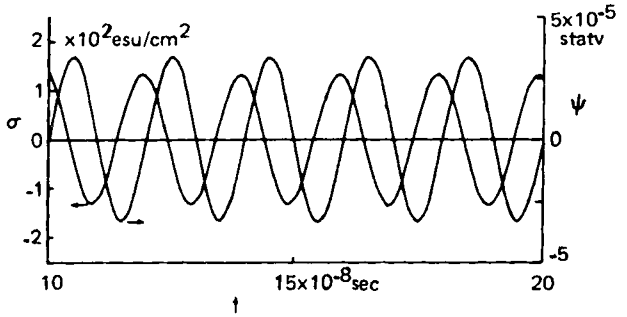

FIG. 4. Response of $\sigma(t)$ to a small, high-frequency sinusoidal voltage. $\psi = 10$ mV·sin $2\pi\nu t$, $\nu = 50$ MHz, other parameters as in Fig. 2.

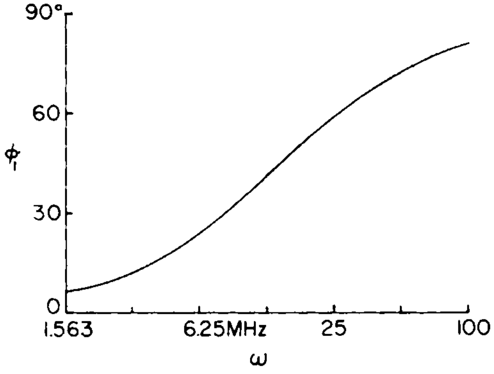

FIG. 5. Dependence of phase angle ϕ_1 of $\sigma(t)$ on applied voltage frequency ν for small voltage amplitude. $\psi(0) = 10$ mV·sin $2\pi\nu t$. ν as indicated, other parameters as in Fig. 2.

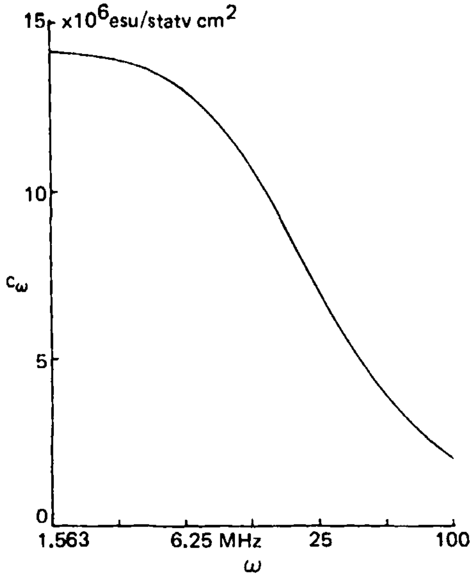

FIG. 6. Dependence of σ_{max} on applied voltage frequency for small voltage amplitude. Parameters as in Fig. 5.

As one increases the amplitude of the input voltage, however, changes in the behavior of $\sigma(t)$ begin to show up. Figure 7 shows a plot of $\sigma(t)$ for $\psi = 300\ (1 + \sin 2\pi\nu t)$ mV, $\nu = 25$ MHz. Here it is qualitatively apparent that the response is no longer a linear function of the input. The flat bottoms and sharper peaks of the plot of $\sigma(t)$ indicate that the differential capacitance is varying substantially with the applied voltage. This nonlinear response is confirmed by the Fourier coefficients given in Table 2; the coefficients of the first harmonic are of the order of 20% of the coefficients of the fundamental. The phase angle is slightly changed (decreased by about 3°) from that found for the low amplitude, linear run. The capacitance for the ac signal has decreased from a value of 0.706×10^7 esu/stat V. cm^2 (for the linear case) to only 0.282×10^7, a decrease by 60%.

These results suggested a more detailed investigation of the effects of the amplitude of the applied voltage at a frequency of 25 MHz. A series of runs were made in which the input voltage was given by $\psi(t) = A(1 + \sin 2\pi\nu t)$, where A ranged from 10 to 300 mV. The results are summarized in Table 3.

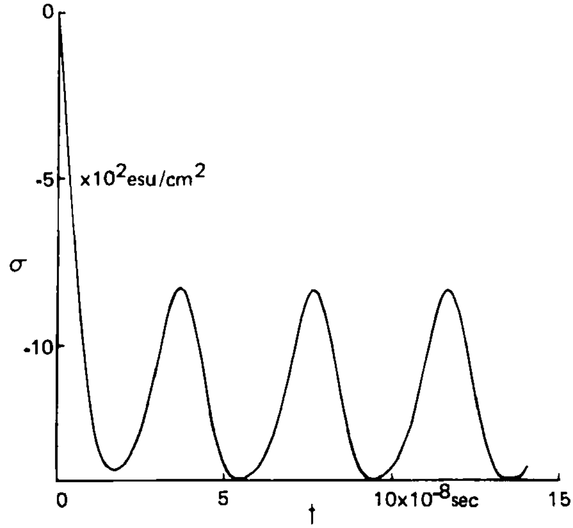

FIG. 7. Response of $\sigma(t)$ to a large sinusoidal voltage. $\psi(0) = 300$ mV$\cdot(1 + \sin 2\pi\nu t)$, $\nu = 25$ MHz, other parameters as in Fig. 2.

We see that the phase angle passes through a maximum of about 68° at $A \cong 150$ mV, and then decreases quite markedly. The ac capacitance shows a uniform and quite substantial decrease with increasing A, falling to half of its low-voltage value at $A \cong 250$ mV. The ratios of the Fourier coefficients of the first harmonic to the amplitude of the fundamental frequency in $\sigma(t)$ show that the first harmonic increases monotonically in amplitude, becoming 10% of the fundamental for A somewhere between 200 and 250 mV.

Let us next look at the effects of varying the effective sizes of the ions. Three runs were made in the nonlinear region ($A = 300$ mV) with $c_{\text{max}} = 5$, 10, and 15 mol/L. The results are given in Table 4. We assume that the effective ionic radius, r, decreases as $(c_{\text{max}})^{-1/3}$. The phase angle decreases with increasing c_{max}, presumably because of the increased mobility of the smaller ions. The values of a_1 and c_ω increase with increasing c_{max}; this is as one would expect, since as c_{max} increases it is possible to get more ions close to the charged surface at $x = 0$. We see a somewhat larger contribution from the first harmonic as c_{max} increases, but can suggest no simple interpretation for this.

TABLE 2
Fourier Coefficients for a Run in the Nonlinear Range
($\nu = 25$ MHz, $\psi_0 = \psi_1 = 300$ mV, other parameters as in Fig. 3)

$c_0 = 0.11668 \times 10^5$ esu/cm^2
$c_1 = 0.15345 \times 10^4$
$s_1 = 0.23178 \times 10^4$
$c_2 = 0.33599 \times 10^3$
$s_2 = 0.40597 \times 10^3$
$c_3 = 0.25882 \times 10^2$
$s_3 = 0.89613 \times 10^1$
$a_1 = 0.27798 \times 10^4$
$\phi_1 = 56.493°$

TABLE 3
Effects of Applied Voltage[a] ($\nu = 25$ MHz, other parameters as in Fig. 3)

A(mV)	ϕ_1 (deg)	$c_\omega \left(\frac{\text{esu}}{\text{stat V cm}^2}\right)$	c_2/a_1	s_2/a_1
10	59.70	0.706×10^7	4.72×10^{-6}	3.28×10^{-4}
50	61.46	0.693	-1.18×10^{-3}	6.59×10^{-3}
100	65.26	0.641	-1.16×10^{-2}	2.23×10^{-2}
150	67.96	0.545	-3.62×10^{-2}	4.17×10^{-2}
200	67.07	0.436	-7.00×10^{-2}	6.58×10^{-2}
250	62.43	0.346	−0.1019	9.99×10^{-2}
300	56.49	0.282	−0.1209	0.1460

[a] Symbols are defined in the text.

TABLE 4
Effects of Ionic Size
($A = 300$ mV, $\nu = 25$ MHz, $T = 298$ K, |ionic charge| = 1, $c_\infty = 0.03$ mol/L)

$c_{\max}$, mol/L	5	10	15
r, Å	2.5198	2.0000	1.7472
ϕ_1, deg	60.05	56.49	54.04
a_1, esu/cm^2	0.228×10^4	0.279	0.310
c_ω, esu/stat V cm^2	0.231×10^7	0.282	0.315
c_2/a_1	−0.1109	−0.1209	−0.1206
s_2/a_1	0.1079	0.1460	0.1740

CONCLUSIONS

We have developed a rather realistic nonideal model for the kinetics of changes in ionic atmospheres in the vicinity of a plane inert electrode maintained at a time-dependent potential. Qualitatively, one may assign a time constant of about 7×10^{-8} s to the system. At higher applied voltages (~300 mV), nonlinear effects become quite noticeable, and may be investigated quantitatively by Fourier analysis. The effective volumes of the ions produces marked effects on the phase angle of the response, the magnitude of the differential capacitance, and the magnitude of the contribution from the first harmonic.

Our results indicate that one can regard the ionic atmospheres in the vicinities of charged, rising bubbles as in equilibrium with the charge on the bubble surface and with the bulk solution. (The time scale for significant bubble motion with respect to the solution, t_b, is of the order of bubble radius/bubble rise velocity,

$$t_b \cong \frac{9\eta}{2g\rho r} = 9.2 \times 10^{-4} \text{ s}$$

for a bubble of radius 0.05 cm in water. The time scale for ionic atmosphere changes, about 7×10^{-8} s, is some four orders of magnitude less.)

The extension of this approach to solutions containing reactive ions in contact with active electrodes might be of interest in giving insight to the processes occurring in the flotation of sulfides with xanthates, in which redox reactions occur.

Acknowledgment

This work was supported by a grant from the National Science Foundation.

REFERENCES

1. F. Sebba, *Ion Flotation*, Elsevier, Amsterdam, 1962.
2. R. Lemlich (ed.), *Adsorptive Bubble Separation Techniques*, Academic, New York, 1972.
3. J.-H. Tzeng and H. Zeitlin, *Anal. Chim. Acta, 101*, 71 (1978).
4. Y. S. Kim and H. Zeitlin, *Ibid., 46*, 118 (1969).
5. E. H. DeCarlo, H. Zeitlin, and Q. Fernando, *Anal. Chem., 54*, 898 (1982).
6. E. H. DeCarlo, H. Zeitlin, and Q. Fernando, *Ibid., 53*, 1104 (1981).
7. A. J. Rubin and W. L. Lapp, *Ibid., 41*, 113 (1969).

8. D. Bhattacharyya, J. A. Carlton, and R. B. Grieves, *AIChE J.*, *17*, 419 (1971).

9. A. J. Rubin and W. L. Lapp, *Sep. Sci.*, *6*, 357 (1971).

10. J. W. Perez and F. F. Aplan, *AIChE Symp. Ser.*, *71*(150), 34 (1975).

11. T. E. Chatman, S.-D. Huang, and D. J. Wilson, *Sep. Sci.*, *12*, 461 (1977).

12. B. B. Ferguson, C. Hinkle and D. J. Wilson, *Ibid.*, *9*, 125 (1974).

13. R. B. Grieves, in *Treatise on Analytical Chemistry*, Part I, Vol. 5 (P. J. Elving, ed.), Wiley, New York, 1982, Chap. 9.

14. D. J. Wilson and A. N. Clarke, *Sep. Purif. Methods*, *7*, 55 (1978).

15. J. Leja, *Surface Chemistry of Froth Flotation*, Plenum, London, 1982.

16. D. J. Wilson, *Sep. Sci.*, *11*, 391 (1976).

17. D. J. Wilson, *Ibid.*, *12*, 231 (1977).

18. B. L. Currin, F. J. Potter, D. J. Wilson, and R. H. French, *Sep. Sci. Technol.*, *13*, 285 (1978).

19. D. J. Wilson, *Ibid.*, *17*, 1219 (1982).

20. J. M. Brown and D. J. Wilson, *Ibid.*, *16*, 773 (1981).

21. J. E. Kiefer and D. J. Wilson, *Ibid.*, *15*, 57 (1980).

22. R. M. Kennedy and D. J. Wilson, *Ibid.*, *15*, 1339 (1980).

23. S.-D. Huang and D. J. Wilson, Sep. Sci., *10*, 405 (1975).

24. P. W. Atkins, *Physical Chemistry*, 2nd ed., Freeman, San Francisco, 1982, p. 798.

25. R. C. Weast (ed.), *Handbook of Chemistry and Physics*, 45th ed., CRC Press, Cleveland, Ohio, p. E36.

Received by editor January 14, 1983